[illegible] lots of import data [illegible]

Journal of Chromatography B, 944 (2014) 55–62

Contents lists available at ScienceDirect

Journal of Chromatography B

journal homepage: www.elsevier.com/locate/chromb

Adduct formation in liquid chromatography-triple quadrupole mass spectrometric measurement of bryostatin 1

Thomas J. Nelson*, Abhik Sen, Daniel L. Alkon, Miao-Kun Sun

Blanchette Rockefeller Neurosciences Institute, 8 Medical Center Drive, Morgantown, WV 26505, USA

ARTICLE INFO

Article history:
Received 2 May 2013
Accepted 10 November 2013
Available online 16 November 2013

Keywords:
Mass spectrometry
Bryostatin 1
Paclitaxel
Adduct
Alzheimer's disease
LC–MS

ABSTRACT

Bryostatin 1, a potential anti-Alzheimer drug, is effective at subnanomolar concentrations. Measurement is complicated by the formation of low *m/z* degradation products and the formation of adducts with various cations, which make accurate quantitation difficult. Adduct formation caused the sample matrix or mobile phase to partition bryostatin 1 into products of different mass. Degradation of the 927 $[M+Na]^+$ ion to a 869 *m/z* product was strongly influenced by ionization conditions. We validated a bryostatin 1 assay in biological tissues using capillary column HPLC with nanospray ionization (NSI) in a triple-quadrupole mass spectrometer in selected reaction monitoring (SRM) mode. Adduct formation was controlled by adding 1 mM acetic acid and 0.1 mM sodium acetate to the HPLC buffer, maximizing the formation of the $[M+Na]^+$ ion. Efficient removal of contaminating cholesterol from the sample during solvent extraction was also critical. The increased sensitivity provided by NSI and capillary-bore columns and the elimination of signal partitioning due to adduct formation and degradation in the ionization source enabled a detection limit of 1×10^{-18} mol of bryostatin 1 and a LLOQ of 3×10^{-18} mol from 1 μl of sample. Bryostatin 1 at low pmol/l concentrations enabled measurement in brain and other tissues without the use of radioactive labels. Despite bryostatin 1's high molecular weight, considerable brain access was observed, with peak brain concentrations exceeding 8% of the peak blood plasma concentrations. Bryostatin 1 readily crosses the blood–brain barrier, reaching peak concentrations of 0.2 nM, and specifically activates and translocates brain PKCε.

1. Introduction

Bryostatin 1 (Fig. 1**a**) is a macrocyclic lactone extracted from *Bugula neritina*, a marine bryophyte [1,2]. Bryostatin 1 is the most abundant of numerous bryostatins, which are synthesized by bacteria that exist in a symbiotic relationship with the bryophyte [3]. Bryostatin 1 is a potent activator of protein kinase C (PKC), particularly the ε and α isozymes, with a K_d of 1.4 nM [4], and binds to the C1a and C1b domains, competing with the natural ligand, diacylglycerol [5–7].

Early studies on bryostatin 1 suggested possible benefits of moderate to high doses, which produce mainly downregulation of PKC, as anti-tumor agents [8–10]. However, clinical trials of bryostatin 1, both alone and in combination with conventional anti-cancer drugs including 1-β-D-arabinofuranosylcytosine [11], cisplatin [12], and paclitaxel [13], have so far shown little or no clinical benefit. This may be attributable to our incomplete understanding of the roles of various PKC isozymes in cancer, or to an incomplete understanding of the dynamics of differential activation and downregulation of PKC isozymes by bryostatin 1 and other C1a/C1b activators at different concentrations.

Bryostatin 1 also shows some promise as a possible treatment for neurodegenerative diseases such as Alzheimer's disease (AD). In Tg2576 transgenic mice, used as a model for AD, bryostatin 1 improves learning in Morris water maze tasks. Activators of PKCε such as bryostatin 1 have demonstrated neuroprotective activity in animal models of AD [14], depression [15], and stroke [16], and can protect or enhance memory in rodents, rabbits, and invertebrates [15,17–19]. This memory enhancement is accompanied by increase in levels of synaptic proteins and structural changes in synaptic morphology [20]. PKCε also reduces Aβ levels by activating Aβ-degrading enzymes including endothelin-converting enzyme [21,22]. Thus, PKCε activators may be an effective adjunct to Aβ-reduction therapy. PKCε activators also induce synaptogenesis in the CA1 stratum radiatum of the dorsal hippocampus of young adult rats [20]. The mechanism of synaptogenesis involves arachidonic acid signaling through PKC, triggered by integrin receptors and astrocytic factors [23]. PKCε also mediates the neuroprotective effects of ApoE/cholesterol [24], which is a synaptogenic signal

---

Abbreviations: LLOQ, lower limit of quantitation; PKC, protein kinase C; AD, Alzheimer's disease; Aβ, beta-amyloid peptide; MTBE, methyl t-butyl ether; NSI, nanospray ionization.

* Corresponding author. Tel.: +1 304 293 0930; fax: +1 304 293 7536.
E-mail address: tjnelson@brni-jhu.org (T.J. Nelson).

1570-0232/$ – see front matter © 2013 Elsevier B.V. All rights reserved.
http://dx.doi.org/10.1016/j.jchromb.2013.11.020

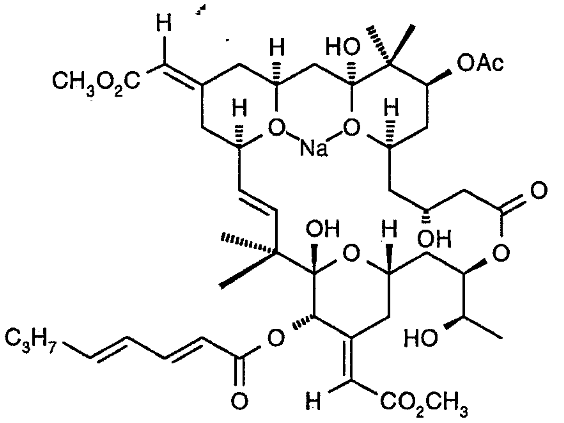

1 $C_{47}H_{68}O_{17}Na$ m/z 927.43

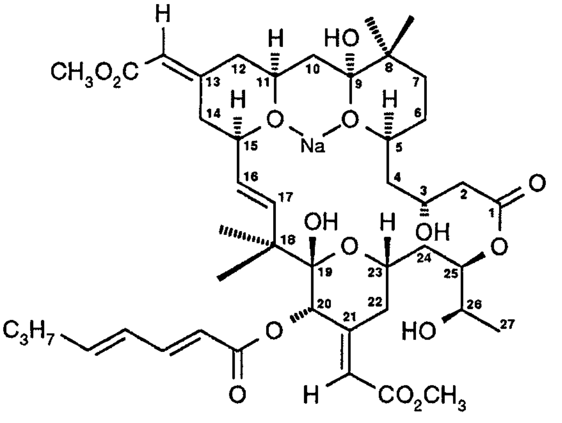

2 $C_{45}H_{66}O_{15}Na$ m/z 869.43

Fig. 1. Structures of bryostatin 1 derivatives. **1** Bryostatin 1 sodium adduct (monoisotopic mass, 927.44; average molecular weight 928.02). **2** the 869.43 (monoisotopic m/z) product proposed by Manning et al. [2].

secreted by astrocytes [25]. These results indicate that activation of endogenous PKCε protects against synaptic loss and facilitates synaptogenesis.

Before proceeding to clinical trials, it is necessary to obtain a clear understanding of the pharmacokinetics of bryostatin 1 and its time- and concentration-dependent effects on various PKC isozymes. Because bryostatin 1 is effective at subnanomolar concentrations, these experiments require highly sensitive assays. Zhao et al. [26] used a triple quadrupole mass spectrometer to detect bryostatin 1 with a LLOQ of 55 pM. Fluorescence derivatization methods have also been developed [27]. However, to achieve adequate sensitivity for animal experiments and clinical trials of bryostatin 1, where sample sizes are limited, even higher levels of sensitivity are required. In this article, we report that control of adduct formation and artifactual degradation in the ionization source are essential to obtaining accurate quantitative measurements of bryostatin 1 in biological samples.

2. Materials and methods

Materials—Bryostatin 1 was obtained from Tocris Bioscience (R&D Systems, Minneapolis, MN, USA). Acetonitrile was obtained from ThermoFisher. Paclitaxel, MTBE, and other chemicals were obtained from Sigma–Aldrich.

2.1. Enzyme assays

Protein kinase C assay—Cells were scraped in 0.2 ml homogenization buffer (20 mM Tris-HCl, pH 7.4, 50 mM NaF, 1 μg/ml leupeptin, and 0.1 mM PMSF) and homogenized by sonication in a Marsonix microprobe sonicator (5 s, 10 W). To measure PKC, 10 μl of cell homogenate or purified PKC isozyme was incubated for 15 min at 37 °C in the presence of 10 μM histones, 4.89 mM $CaCl_2$, 1.2 μg/μl phosphatidyl-L-serine, 0.18 μg/μl 1,2-dioctanoyl-sn-glycerol, 10 mM $MgCl_2$, 20 mM HEPES (pH 7.4), 0.8 mM EDTA, 4 mM EGTA, 4% glycerol, 8 μg/ml aprotinin, 8 μg/ml leupeptin, and 2 mM benzamidine. 0.5 μCi·[γ^{32}P]ATP was added and ^{32}P-phosphoprotein formation was measured by adsorption onto phosphocellulose as described previously [28].

For measurements of activation by bryostatin 1 and similar compounds, PKC activity was measured in the absence of diacylglycerol and phosphatidylserine, as described by Kanno et al. [29], and PKCδ, ε, and α were measured in the absence of added EGTA and $CaCl_2$, as described by Kanno et al. [29]. Low concentrations of Ca^{2+} are used because high Ca^{2+} interacts with the PKC phosphatidylserine binding site and prevents activation. For measurements of bryostatin 1 activation, 1,2-diacylglycerol was omitted unless otherwise stated.

PKC isozyme translocation—Activation and translocation of PKCε were measured by western blotting after subcellular fractionation into cytosol and particulate fractions. Homogenates were centrifuged at 100,000 × g for 20 min and cytosolic and particulate fractions were separated on 4–20% Tris–glycine SDS polyacrylamide gels, blotted onto nitrocellulose, and probed with isozyme specific antibodies. The blots were photographed in a GE ImageQuant at 16 bits/pixel and analyzed by vertical strip densitometry using Imal Unix software.

2.2. Sample preparation and bryostatin 1 measurement

Bryostatin 1 extraction from tissue—Tissue samples were sonicated in 2 vol. of homogenization buffer (30 s, 10 W), and 0.1–0.5 ml homogenate was extracted 2× with 0.3 ml methyl t-butyl ether (MTBE) and methanol as described below for extraction from blood plasma.

Bryostatin 1 Extraction from blood plasma—Blood plasma was extracted using a modification of the MTBE-methanol method of Matyash et al. [30]. Methanol (100 μl) and MTBE (300 μl) were added to 100 μl EDTA-treated blood plasma in a 1.5-ml polypropylene centrifuge tube. The sample was vortexed and centrifuged for 10 min at 15,000 × g. The upper phase was transferred to a new 1.5-ml polypropylene centrifuge tube, 300 μl MTBE were added, the sample was vortexed and centrifuged again, and the upper phase was combined with the first extraction. The sample was evaporated to dryness by evaporation under nitrogen in a water bath at 50 °C. The sample was then redissolved in 0.1 ml ethanol and vortexed. The ethanol was evaporated to dryness and the sample was redissolved in 0.1 ml 50% acetonitrile in water, centrifuged for 1 min at 11,000 × g, and transferred to a glass-insert mass spectrometry vial. Samples were stored at −20 °C until use, warmed in a 37 °C water bath, and vortexed before loading onto the autosampler, which was maintained at 25 °C.

— plasma or serum?

Sample quantities— For serum samples, 100 μl serum was used. For brain samples, 0.5 ml of 1→3 homogenate, containing approximately 166 μg protein, was used. The MTBE/methanol extracts of samples and standards were dissolved in 100 μl of 50% acetonitrile in water and the entire sample was transferred to an autosampler vial containing a 0.2 ml glass insert and Teflon screw-cap. A 1.0 μl aliquot was injected for all samples. Quantitation results are reported either as mol measured in the 1 μl that was injected onto the LCMS instrument, or as mol/liter or mol/kg of original tissue, as appropriate, except where noted.

seems like plasma.

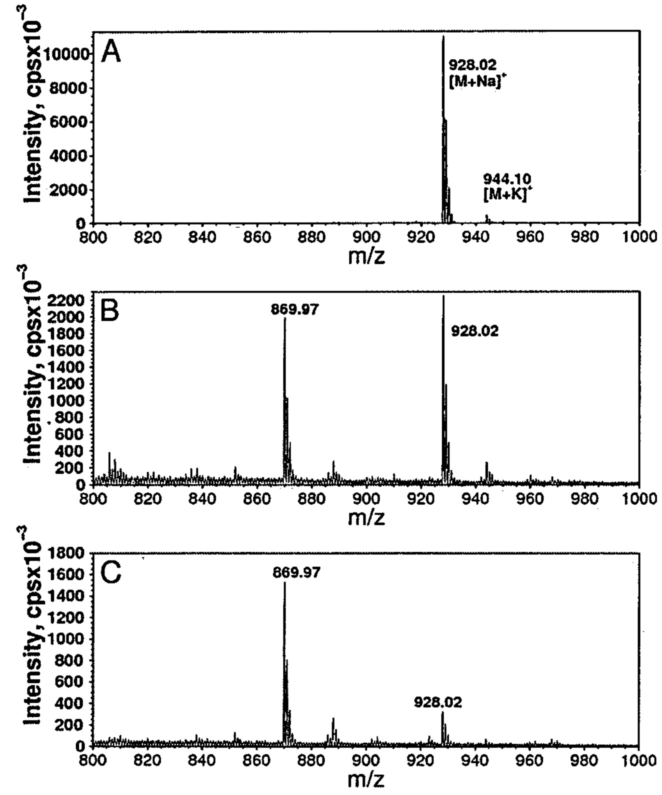

Fig. 2. Mass spectra of bryostatin 1 solution in ethanol in NSI spray with (A) normal spray, (B) spray offset vertically by 1 mm, and (C) spray offset by 2 mm. Offsetting the spray greatly increased the size of the 869 *m/z* peak at the expense of the 927 *m/z* peak. Increasing the spray voltage above 2350 V had the same effect. Average molecular weights are shown.

results. These results suggest that the 869 peak is not a photooxidation product, but a fragmentation product formed in the ESI source under unfavorable spray conditions. The matrix effects suggest that cation complexation may protect bryostatin 1 from degradation.

3.2. *Adduct formation*

It is evident that this partitioning of the signal among different masses depending on matrix composition would seriously impair the reliability of quantitation. Quantitation of the anticancer drug paclitaxel is plagued by similar issues, and adduct formation splits the paclitaxel signal into Na^+, K^+, H^+, and NH_4^+ adducts with different masses [33–35]. Reproducibility is reportedly enhanced by the addition of octylamine to the LC buffers. Therefore, we tested a variety of solvent additives to identify optimal conditions for quantitation of bryostatin 1 in biological tissues. The results are shown in Table 1. Octylamine, tetramethylethylenediamine (TEMED), dodecylamine, and *n*-propylamine were found to form adducts with bryostatin 1. By contrast, pyridine did not form an adduct but increased the size of the 869 degradation product peak to 33% of the total, and ethanolamine abolished all bryostatin 1 peaks. However, no additive was completely effective in displacing sodium from bryostatin 1. Acidification of bryostatin 1 solutions with HCl resulted in degradation. The $[M+H]^+$ ion was not observed under any conditions.

The bryostatin 1-Na^+ adduct could also be disrupted by incubating with 15-crown-5 (Fig. 3). A 5-fold excess was required, indicating that bryostatin 1 binds Na^+ with high affinity. Bryostatin 1 was partially shifted to numerous lower *m/z* peaks (*m/z* 450–600, not shown) in the presence of 15-crown-5, suggesting that cation complexation may be important for stability. Addition of 1 mM potassium acetate to bryostatin 1 resulted in K^+ completely displacing Na^+ from bryostatin 1, leaving only the 943.41 *m/z* bryostatin 1-K^+ adduct in the expected isotopic ratios (Fig. 3).

Table 1
Adduct formation between bryostatin 1 and amines. In all cases, except for ethanolamine and pyridine, the total peak height (927 peak + expected peak) was not affected. For ethanolamine, no bryostatin 1 peaks were detected. For pyridine, the 927 peak was shifted to 869.

Additive	Expected *m/z*	Relative signal at expected *m/z* (%)
Ammonium carbonate (10 mM)	921	0
n-propylamine	964	25
Ethanolamine	966	ND
Pyridine	984	0
1,2-diaminopropane	979	0
Triethylamine	1006	9
TEMED (tetramethylenediamine)	1021	20
2-diethylaminopyridine	1027	0
Tri-*n*-butylamine	1090	0
Octylamine	1034	50
Dodecylamine	1090	25
Trioctylamine	1258	0

Amines were added to bryostatin 1 dissolved in 50% acetonitrile at a concentration of 1% (v/v), except for ammonium carbonate, which was added at 10 mM; ND, not detected.

No peaks were observed for free bryostatin 1 or bryostatin 1 adducts in negative ion mode using standard buffers. However, addition of bases such as pyridine, 2-(dimethylamino)pyridine, octylamine, and 1,2-diaminopropane allowed the detection of the *m/z* 903.44 $[M-H]^-$ parent ion in negative ion mode, but the signal was always 100–300× lower than the bryostatin 1 signal in positive ion mode.

3.3. *LC conditions*

As reported for paclitaxel [35], addition of acetic acid also increased the sensitivity for bryostatin 1. In the case of bryostatin 1, acetic acid increased the signal by 5.25-fold. Therefore, we used a gradient of 80% buffer A (1 mM acetic acid + 0.1 mM sodium acetate in water) to 80% buffer B (1 mM acetic acid in acetonitrile) to improve sensitivity by maximizing the Na^+ adduct [36]. Under these conditions, formation of the 869 peak was suppressed to less than 2% of the total, reproducible quantitation was

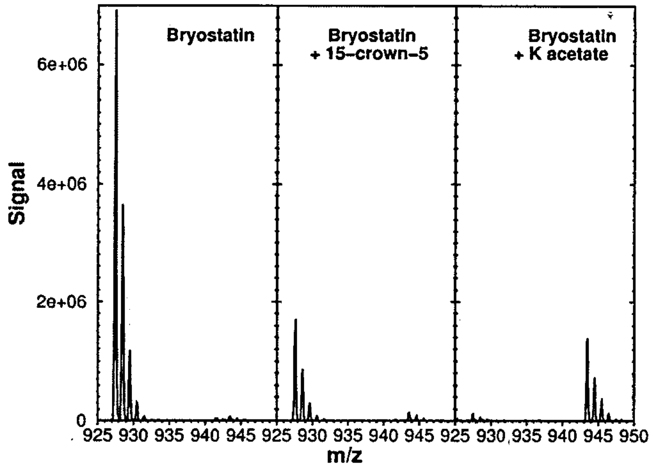

Fig. 3. Disruption of bryostatin 1-sodium adduct. **Left:** bryostatin 1 (2 μM) in ethanol alone. **Center:** bryostatin 1 incubated with 15-crown-5 (10 μM) for 72 h at room temperature. Chelation of Na^+ by crown ethers reduced the bryostatin 1 signal. **Right:** Bryostatin-K+ adduct formed immediately after addition of 1 mM potassium acetate to bryostatin 1 in ethanol.

Table 2
LS-nanospray ESI-MS/MS parameters for quantitation of bryostatin 1.

Parameter	Paclitaxel	Bryostatin 1
Retention time (min)	21.23	29.42
SRM transition (*m/z*)	876.83→308.39	927.44→357.32
Width (*m/z*)	0.010	0.010
CID (mTorr)	1.8	1.8
CE (V)	40	55

Table 3
Extraction efficiency of various solvents.

Solvent	Efficiency for bryostatin 1	Efficiency for cholesterol
MTBE only (1 extraction)	7.4 ± 0.8	ND
MTBE/methanol 3:1 (1 extraction)	103.9 ± 3.2	ND
MTBE only (2 extractions)	34.6 ± 7.5	0.75 ± 0.11
MTBE/methanol 3:1 (2 extractions)	97.7 ± 6.3	1.3 ± 0.3
ACN/1-chlorobutanol 1:1	102.2 ± 4.1	2.1 ± 0.8
Toluene/ethanol 3:1	109.9 ± 12.7	3.4 ± 1.3
Ethyl acetate	33.0 ± 3.1	1.1 ± 0.34
Ethyl acetate/hexane 3:1	34.2 ± 3.0	0.77 ± 0.07
Hexane	6.0 ± 2.0	ND
Chloroform/methanol 2:1	19.0 ± 2.1	0.56 ± 0.05

Bryostatin 1 (2 pmol) and cholesterol (0.5 µmol) were extracted 2× from 0.1 ml serum samples using 0.3 ml of the indicated solvent. Bryostatin 1 was measured by LCMS/NSI. Cholesterol was measured by infusion and APPI. Numbers are mean ± SD of 3 determinations. ND, not determined.

obtained, and syringe infusion signals finally matched the signals from C18 columns. Accordingly, we used selected reaction monitoring (SRM) of the 927.44→357.32 transition in all experiments. The 876.83→308.39 transition of paclitaxel was used as an internal standard. Paclitaxel is slightly more polar than bryostatin 1 (t_R 21.23 vs. 29.42 min, Table 2), and is ideal as an internal standard because its MW and polarity are similar to bryostatin 1. A SRM chromatogram of bryostatin 1 extracted from mouse brain is shown in Fig. 4.

3.4. Extraction

For preclinical measurements, an important consideration is the ability to separate bryostatin 1 from unesterified cholesterol, which exists in brain at a 5×10^8-fold excess (58 mM [37] vs. 0.1 nM). These high levels of cholesterol in brain would preclude the use of nano- and capillary-columns because of cholesterol's limited solubility in the chromatography buffer. Large quantities of cholesterol would precipitate in the 50% acetonitrile solution or in the column itself, mandating the use of more dilute samples and larger diameter columns. This is not a problem for blood plasma, but could severely affect sensitivity with tissue samples. Therefore, several different extraction techniques were compared. Table 3 shows that toluene/ethanol, acetonitrile/1-chlorobutane, and MTBE/methanol were the most effective solvents for bryostatin 1, while other extraction solvents, including pure MTBE, chloroform/methanol, hexane, and ethyl acetate, were less efficient. A single extraction with MTBE/methanol was as efficient as two extractions. If two extractions are performed, methanol can be omitted during the second extraction to reduce aqueous carry-over, but methanol was essential during the first extraction. The low solubility of cholesterol in 50% acetonitrile/water solutions (<1 µM) was instrumental in reducing cholesterol to manageable levels.

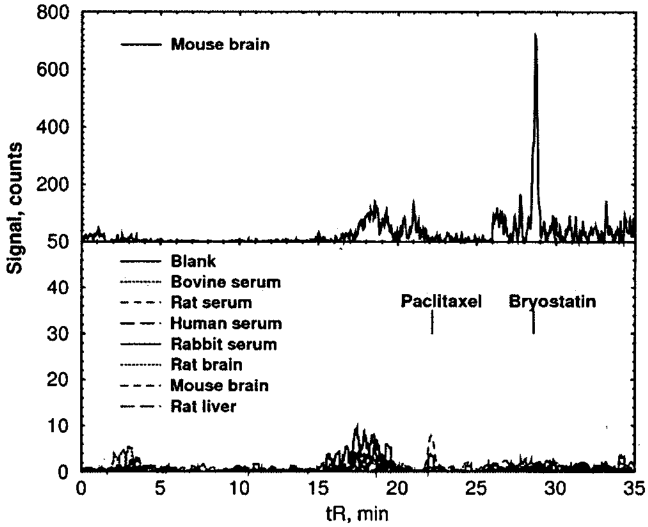

Fig. 4. Top: SRM chromatogram of bryostatin 1 extracted from mouse brain 6 h after injection with bryostatin 1 at a dose of 15 µg/m². The brain concentration is 0.247 nM. This represents 411 amol of bryostatin 1. **Bottom:** Lack of interference from sample matrix in control samples extracted from bovine, rat, human, or rabbit serum or rat brain, mouse brain, or rat liver.

3.5. Validation

The LLOQ using nanospray and a 50 mm × 180 µm (i.d.) column, with 1 µl injection, was 3 amol, corresponding to a concentration in the autosampler of 3 pM (Fig. S1). The increase in sensitivity provided by NSI and capillary-bore columns permits bryostatin 1 measurements from small quantities of plasma or brain tissue. The highest two samples in Fig. S1 contain only 3 repetitions instead of 12 due to sample limitations. At these concentrations, the signal approached the saturation point of the detector's ADC (2.59×10^8 counts). The chromatographic peak also became highly asymmetrical when measuring quantities >10 pmol. The sensitivity was critically dependent on the efficiency of the chromatography step. Shortening the analysis time using isocratic 90% acetonitrile and a flow rate of 3 µl/min resulted in a shorter retention time (4.5 vs. 28 min) but also greater noise and no significant reduction in peak width. This raised the LLOQ of a 1 µl sample to 40 amol and the limit of detectability to 10 amol, giving a minimum measurable concentration in the 100 µl sample vials of 40 pM (not shown).

Supplementary material related to this article can be found, in the online version, at http://dx.doi.org/10.1016/j.jchromb.2013.11.020.

The coefficients of variation for intra-batch and inter-batch precision for bryostatin 1 extracted from blood serum were within 15% (Table 4). Mean values were within 15% of expected values for all concentrations between 3×10^{-18} and 3×10^{-12} mol per injection.

Previous researchers found that bryostatin 1 is stable for over three weeks at 50 °C in daylight or 30 weeks at −20 °C [24,38] but had a tendency to adsorb onto poly(vinyl chloride) [39]. We found that bryostatin 1 in glass or polypropylene tubes remains in solution indefinitely when dissolved in ethanol. However, bryostatin 1 was lost when heated to dryness in glass tubes or allowed to evaporate to dryness overnight in glass containers. Therefore,

Table 4
Accuracy, precision, and recovery of bryostatin 1 extraction from blood serum by MTBE/methanol.

Concentration (µM)	Quantity (fmol)	RSD (%)	Precision	
			Intra-batch	Inter-batch
0.002	2	1.68	101.6	107.0
0.02	20	2.99	101.7	97.3
0.2	200	2.99	103.4	105.4

RSD, relative standard deviation expressed as percent of mean value. Inter-batch precision is based on 3 different experiments. Intra-batch precision is based on 3 concentrations and 6 samples each.

Table 5
Stability of bryostatin 1.

Short-term stability	2 h	8 h	24 h
Stock RT high	100.0 ± 4.6	104.0 ± 3.1	88.3 ± 1.3
Stock RT low	100.0 ± 2.3	107.6 ± 2.5	81.5 ± 1.9
Short term RT high	100.0 ± 4.4	108.0 ± 11.3	92.7 ± 1.8
Short term RT low	101.0 ± 3.0	105.2 ± 5.5	99.8 ± 4.4

Long-term stability	0d	1d	2d	4d	7d
Autosampler RT high	100.0 ± 1.7	94.8 ± 15	103.1 ± 8.6	99.2 ± 2.6	97.8 ± 15
Autosampler RT low	102.0 ± 3.0	99.8 ± 5.1	110.1 ± 4.7	111.8 ± 9.9	86.6 ± 10.5

Long-term stability	1d	3d	7d	21d
−80 °C high	103.3 ± 10.5	87.5 ± 7.4	84.1 ± 8.6	85.2 ± 7.6
−80 °C low	94.1 ± 4.0	98.0 ± 6.6	120.5 ± 6.2	89.9 ± 6.4

Multiple Freeze-thaw high	100.8 ± 1.1
Multiple Freeze-thaw low	106.5 ± 0.8

Stability testing was done as prescribed in FDA Guidance documents. Numbers are mean recovery ± SD for 3–5 determinations. High concentration, 100 nM; low concentration, 10 nM except stock solution, high concentration = 10 μM, low concentration = 100 nM. Multiple freeze-thaw samples were freeze-thawed 3× from −80 °C to room temperature.

all operations involving evaporation were carried out in polypropylene tubes. Bryostatin 1 is stable to base, with no degradation observed after 5 min boiling in concentrated pyridine or 10% 4-dimethylaminopyridine in ethanol. Treatment with 1% methanolic KOH for 10 s at room temperature did not cause noticeable degradation or dissociation of the Na^+ adduct. Bryostatin 1 was rapidly degraded under acidic conditions (0.2 M HCl, room temperature, 1 min).

To determine the thermal stability of bryostatin, we incubated samples at various temperatures and times in an oxygen-free environment, and then measured the remaining bryostatin by normal-phase HPLC. Bryostatin 1 was found to be rapidly degraded at temperatures exceeding 170 °C; its $t_{1/2}$ was 10 min at 180 °C and 5 min at 190 °C. Since bryostatin 1's melting point is reported to be 230–235 °C, this precludes analysis of bryostatin 1 by gas chromatography or GCMS. ~~Bryostatin 1 stability results are shown in Table 5.~~ Recovery and interference results are shown in Table 6. Recovery showed no dependence on species or tissue. Bovine serum, rat serum, rabbit serum, human serum, and rat brain had no effect on recovery. Other drugs potentially present in Alzheimer patients, measured at 1× and 10× therapeutic concentrations, including captopril (therapeutic concentration, 50 μM), acetaminophen (150 μM), memantine (1 μM), donepezil (1 μM), galantamine (1 μM), and tacrine (1 μM) also produced no detectable interference either with bryostatin or paclitaxel (Fig. S2). Extraction from several sources of control blood plasma, as well as rat brain, mouse brain, and rat liver, showed no interference from any sample matrix tested, only noise peaks at levels below the detection limit (Fig. 4, lower panel).

Supplementary material related to this article can be found, in the online version, at http://dx.doi.org/10.1016/j.jchromb.2013.11.020.

Table 6
Recovery and interference.

Bryostatin 1 only	100.0 ± 2.1
+ Bovine serum	107.5 ± 2.1
+ Rat serum	99.0 ± 4.2
+ Rabbit serum	104.7 ± 18.3
+ Human serum	93.3 ± 6.8
+ Rat brain	98.0 ± 12.6

Recovery testing was done as prescribed in FDA guidelines. Numbers are mean recovery ± SD for 3–5 determinations. Bryostatin = 1 fmol; serum = 100 μl; rat brain homogenate = 100 μl.

3.6. In vivo pharmacokinetics and pharmacodynamics of bryostatin 1

To test the ability of the method to obtain meaningful pharmacokinetic data in a preclinical experiment, we conducted PK/PD experiments in mice to determine the plasma concentrations necessary to activate PKCε. Bryostatin 1 was injected into the tail vein of C57BL/6N mice at 10 and 15 μg/m² (equivalent to 3.50 and 5.25 μg/kg), and bryostatin 1 levels were determined as a function of time (Fig. 5). The half-lives of bryostatin 1 in blood plasma and brain, estimated using Marquardt least squares analysis, were estimated at 3.5 ± 0.6 (mean ± SD) and >10 h, respectively. The brain concentrations at the two different doses were not significantly different, suggesting that brain uptake is saturated at doses of 10 μg/m². The maximum brain concentration that could be achieved by any dose was 0.20 nM. Peak brain concentrations were 15.3% and 8.1% of the peak plasma concentrations. At 4 h, the brain concentrations at 10 and 15 μg/m² were 42% and 30% of the respective plasma concentrations. This is in general agreement with the results of Zohar et al. [40] and Zhang et al. [41], where peak brain

? rate differs between [illegible]

Apparent non-linear Cmax?

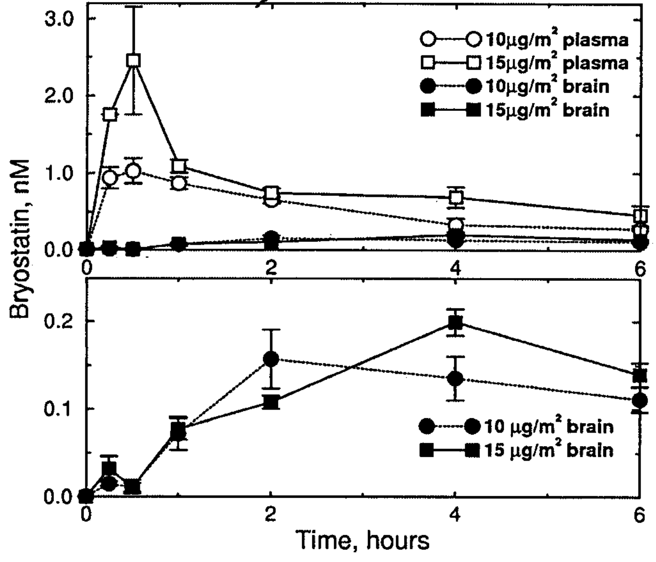

no delay & then [illegible]

Fig. 5. Time course of bryostatin 1 concentration in mouse brain and blood plasma after injection of bryostatin 1 (10 or 15 μg/m² in lateral tail vein). In the lower panel the brain data are re-plotted on a different scale for clarity.

? protein binding
or RBC partition?
but simplistically probably ~1–
seek Cmax ~2 nM in plasma = ng/mL

RDS – need Cmax est for probable [illegible] ng/ml dosing

?

not statistically, but presumably whole brain homogenate; although the effect is [illegible] in brain (1 dose)

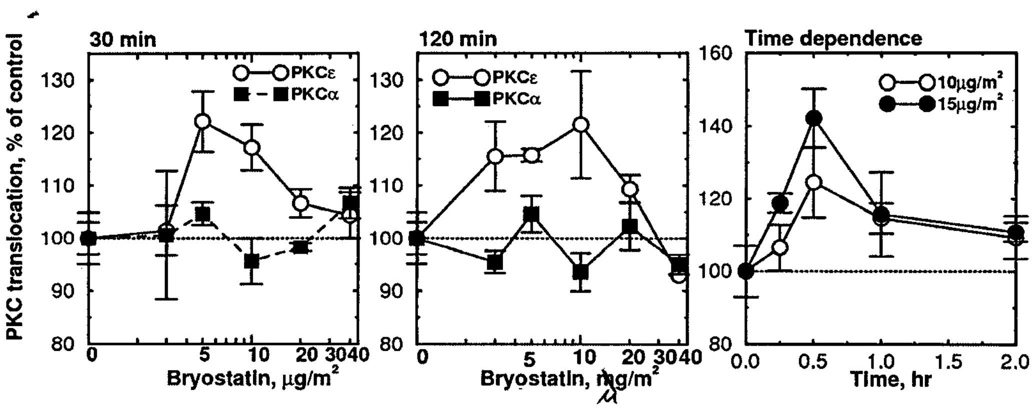

Fig. 6. **Left, Center** = Dose-dependence of activation of PKCα and PKCε translocation by bryostatin 1, measured 30 min and 120 min after administration of 15 μg/m² bryostatin 1 by i.v. in the lateral tail vein. **Right** = time dependence of PKC activation at 10 and 15 μg/m².

^{3}H from labeled bryostatin 1 ranged from 10 to 40% of peak blood plasma concentrations.

Brain PKCε activation, as expected, was biphasic, peaking at 0.5 h and slowly declining toward resting levels, even though bryostatin 1 levels continued to increase (Fig. 6). This is consistent with the short-lived activation of PKC observed previously with bryostatin. No downregulation below starting values was observed. The brain bryostatin 1 concentration at 0.5 h was 0.029 nM.

The effect of bryostatin 1 on brain PKC translocation (an indicator of enzymatic activation) was also biphasic, with maximal effects observed at 30–120 min and doses between 5 and 10 μg/m² (Fig. 6). In contrast to *in vitro* measurements with purified PKC isozymes, for which bryostatin 1 activates the α and ε isoforms equally [42], in mouse brain translocation was only observed for PKCε. The preference for ε over α has also been observed by other researchers [43,7].

4. Discussion

The ring structure of bryostatin 1 closely resembles that of crown ethers, raising the possibility that in addition to activating PKC, bryostatin 1 may also play a biological role in regulating the concentrations of sodium, potassium, or other cations such as Fe^{3+} [31,44]. Bryostatin 1 has a much higher affinity for sodium than paclitaxel, and addition of primary amines was not effective in displacing metal cations from bryostatin 1 under our conditions. Addition of sodium acetate to the buffer is therefore essential in suppressing the formation of different cation adducts in ratios dependent on the composition of the sample matrix, which would cause unacceptable variability in quantitation. Precise control of the electrospray conditions is also essential in preventing bryostatin 1 from partitioning between the 927 and 869 *m/z* species. Efficient removal of contaminating cholesterol from the sample is also critical in allowing bryostatin 1 to be extracted in a volume small enough to enable the use of narrow-bore columns and small sample volumes. This in turn permits the detection of bryostatin 1 at pmol/l concentrations, enabling measurement of bryostatin 1 in brain and other tissues for the first time without the use of radioactive labels.

With low flow rates, injecting small amounts of sodium acetate through a nanospray source does not cause problems, provided that the inlet is washed periodically with water. However, at larger flow rates, it may be desirable to avoid sodium-containing buffers. Although we saw no signal with ammonium-containing buffers under our conditions, one commercial laboratory reported that bryostatin 1-$NH4^+$ adducts were detectable in a Sciex API-4000 triple quadrupole mass spectrometer using a Turbo-ionspray source when the source temperature is kept below 250 °C, the cone voltage is reduced, and high concentrations (2–10 mM) ammonium acetate or ammonium formate are used (Dale Schoener, Intertek, personal communication). Thus, for instruments using higher flow rates, ammonium-containing buffers may be preferable to sodium.

In mouse brain, bryostatin 1 specifically activates PKCε; however, its therapeutic window of efficacy is remarkably narrow due to PKC downregulation at high doses. Despite its high molecular weight, considerable brain access was observed, with peak brain concentrations exceeding 8% of the peak blood plasma concentrations. Our results demonstrate that bryostatin 1 at low doses crosses the blood–brain barrier and activates and translocates brain PKC. At higher doses, activation is not observed due to downregulation, but no doses were found at which downregulation reduces PKC activity in brain to below normal levels.

References

[1] G.R. Pettit, C.L. Herald, D.L. Doubek, D.L. Herald, E. Arnold, J. Clardy, J. Am. Chem. Soc. 104 (1982) 6846.
[2] K.J. Hale, M.G. Hummersone, S. Manaviazar, M. Frigerio, Nat. Prod. Rep. 19 (2002) 413.
[3] S.K. Davidson, S.W. Allen, G.E. Lim, C.M. Anderson, M.G. Haygood, Appl. Environ. Microbiol. 67 (2001) 4531.
[4] P.A. Wender, J.C. Horan, V.A. Verma, Org. Lett. 8 (2006) 5299.
[5] P.S. Lorenzo, K. Bogi, K.M. Hughes, M. Behesthi, D. Bhattacharyya, S.H. Garfield, G.R. Pettit, P.M. Blumberg, Cancer Res. 59 (1999) 6137.
[6] K. Bogi, P.S. Lorenzo, Z. Szallasi, P. Acs, G.S. Wagner, P.M. Blumberg, Cancer Res. 58 (1998) 1423.
[7] P.A. Wender, B. Lippa, C.M. Park, K. Irie, A. Nakahara, H. Ohigashi, Bioorg. Med. Chem. Lett. 9 (1999) 1687.
[8] M. Gschwendt, G. Furstenberger, S. Rose-John, M. Rogers, W. Kittstein, C.L. Pettit, F. Marks, Carcinogenesis 9 (1988) 555.
[9] J. Kortmansky, G.K. Schwartz, Cancer Invest. 21 (2003) 924.
[10] J.L. Marshall, N. Bangalore, D. El-Ashry, M. Johnson, B. Norris, M. Oberst, E. Ness, S. Wojtowicz-Praga, P. Bhargava, N. Rizvi, S. Baidas, M.J. Hawkins, Cancer Biol. Ther. 1 (2002) 409.
[11] L.H. Cragg, M. Andreeff, E. Feldman, J. Roberts, A. Murgo, M. Winning, M.B. Tombes, G. Roboz, L. Kramer, S. Grant, Clin. Cancer Res. 8 (2002) 2123.
[12] R.J. Morgan, L. Leong, W. Chow, D. Gandara, P. Frankel, A. Garcia, H.J. Lenz, J.H. Doroshow, Invest. New Drugs 30 (2012) 723.
[13] A.P. Lam, A.P. Sparano, V. Vinciguerra, A.J. Ocean, P. Christos, H. Hochster, F. Camancho, S. Goel, A. Mani, Kaubisch, Am. J. Clin. Oncol. 33 (2010) 121.
[14] R. Etcheberrigaray, M. Tan, I. Dewachter, C. Kuiperi, I. Van der Auwera, S. Wera, L. Qiao, B. Bank, T.J. Nelson, A.P. Kozikowski, F. Van Leuven, D.L. Alkon, Proc. Natl. Acad. Sci. U S A 10 (2004) 11141.
[15] M.K. Sun, D.L. Alkon, Eur. J. Pharmacol. 512 (2005) 43.
[16] M.K. Sun, J. Hongpaisan, T.J. Nelson, D.L. Alkon, Proc. Natl. Acad. Sci. U. S. A 105 (2008) 13620.
[17] D. Wang, D.S. Darwish, B.G. Schreurs, D.L. Alkon, Behav. Pharmacol. 19 (2008) 245.
[18] A.M. Kuzirian, H.T. Epstein, C.J. Gagliardi, T.J. Nelson, M. Sakakibara, C. Taylor, A.B. Scioletti, D.L. Alkon, Biol. Bull. 210 (2006) 201.
[19] G. Weskamp, J. Schlondorff, L. Lum, J.D. Becherer, T.W. Kim, P. Saftig, D. Hartmann, G. Murphy, C.P. Blobel, J. Biol. Chem. 279 (2004) 4241.
[20] J. Hongpaisan, D.L. Alkon, Proc. Natl. Acad. Sci. U. S. A. 104 (2007) 19751.
[21] T.J. Nelson, C. Cui, Y. Luo, D. Alkon, J. Biol. Chem. 284 (2009) 34514.

[22] D.S. Choi, D. Wang, G.Q. Yu, G. Zhu, V.N. Kharazia, J.P. Paredes, W.S. Chang, J.K. Deitchman, L. Mucke, R.O. Messing, Proc. Natl. Acad. Sci. U. S. A. 103 (2006) 8215.
[23] H. Hama, C. Hara, K. Yamaguchi, A. Miyawaki, Neuron 41 (2004) 405.
[24] A. Sen, D.L. Alkon, T.J. Nelson, J. Biol. Chem. 287 (2012) 15947.
[25] E.M. Ullian, S.K. Sapperstein, K.S. Christopherson, B.A. Barres, Science 291 (2001) 657.
[26] M. Zhao, M.A. Rudek, P. He, B.D. Smith, S.D. Baker, Anal. Biochem. 337 (2005) 143.
[27] T.J. Nelson, Anal. Biochem. 419 (2011) 40.
[28] T.J. Nelson, D.L. Alkon, J. Neurochem. 65 (1995) 2350.
[29] T. Kanno, H. Yamamoto, T. Yaguchi, R. Hi, T. Mukasa, H. Fujikawa, T. Nagata, S. Yamamoto, A. Tanaka, T. Nishizaki, J. Lipid Res. 47 (2006) 1146.
[30] V. Matyash, G. Liebisch, T.V. Kurzchalia, A. Shevchenko, D. Schwudke, J. Lipid Res. 49 (2008) 1137.
[31] T.J. Manning, E. Rhodes, M. Land, R. Parkman, B. Sumner, T.T. Lam, A.G. Marshall, D. Phillips, Nat. Prod. Res. 20 (2006) 611.
[32] T.J. Manning, M. Land, E. Rhodes, L. Chamberlin, J. Rudloe, D. Phillips, T.T. Lam, J. Purcell, H.J. Cooper, M.R. Emmett, A.G. Marshall, Nat. Prod. Res. 19 (2005) 467.
[33] K.A. Mortier, G.F. Zhang, C.H. Van Peteghem, W.E. Lambert, J. Am. Soc. Mass Spectrom. 15 (2004) 585.
[34] K.A. Mortier, V. Renard, A.G. Verstraete, A. Van Gussem, S. Van Belle, W.E. Lambert, Anal. Chem. 77 (2005) 4677.
[35] S. Gao, Z.P. Zhang, L.E. Edinboro, L.C. Ngoka, H.T. Karnes, Biomed. Chromatogr. 20 (2006) 683.
[36] M. Jemal, R.B. Almond, D.S. Teitz, Rapid Comm. Mass Spectrom. 11 (1997) 1083.
[37] J. Dietschy, S.D. Turley, J. Lipid Res. 54 (2004) 1375.
[38] J.C. Baer, J.A. Slack, G.R. Pettit, J. Chromatogr. 467 (1989) 332.
[39] National Cancer Institute, IND 42,780.
[40] O. Zohar, R. Lavy, X. Zi, T.J. Nelson, J. Hongpaisan, C.G. Pick, D.L. Alkon, Neurobiol. Dis. 41 (2011) 329.
[41] X. Zhang, R. Zhang, R. Zhao, H. Cai, K. Gush, R. Kerr, G. Pettit, A. Kraft, Cancer Res. 56 (1996) 802.
[42] M.G. Kazanietz, N.E. Lewin, F. Gao, G.R. Pettit, P.M. Blumberg, Mol. Pharmacol. 46 (1994) 374.
[43] Z. Szallasi, C.B. Smith, G.R. Pettit, P.M. Blumberg, J. Biol. Chem. 269 (1994) 2118.
[44] G. Abadi, T.J. Manning, K. McLeod, D. Phillips, P. Groundwater, L. Noble, T. Potter, Nat. Prod. Res. 22 (2008) 865.